Available online at www.sciencedirect.com
ScienceDirect
Journal of the European Ceramic Society 31 (2011) 1835–1840
www.elsevier.com/locate/jeurceramsoc

Original article

Dynamic behavior of nanometer-scale amorphous intergranular film in silicon nitride by *in situ* high-resolution transmission electron microscopy

Zaoli Zhang [a,b,*], Wilfried Sigle [a], Christoph T. Koch [a], Manfred Rühle [a]

[a] *MPI für Metallforschung, Heisenbergstraße 3, D-70569 Stuttgart, Germany*
[b] *Erich Schmid Institute of Materials Science, Austrian Academy of Sciences, A-8700 Leoben, Jahnstraße 12, Austria*

Received 8 January 2011; accepted 8 March 2011
Available online 8 April 2011

Abstract

We report about the dynamic behavior of a nanometer-scale amorphous intergranular film (IGF) in a Si_3N_4 ceramic by an *in situ* heating experiment in a high-resolution transmission electron microscopy (HRTEM). During the experiment the IGF gradually vanishes at 820 °C accompanied by the formation of crystal planes within the IGF. The IGF reappears after cooling back to room temperature. The results cannot be explained within the framework of a force balance model. We argue that the dynamic behavior of the IGF in our experiment originates from the open system observed.

Keywords: Si_3N_4 ceramic; Intergranular amorphous film (IGF); *In situ* HRTEM; Continuum model

1. Introduction

As structural materials with outstanding high-temperature properties, Si_3N_4-based ceramics have received much attention and their properties have been studied extensively. As a result of liquid phase sintering, grain boundaries other than low- or special (low Σ) angle ones, in Si_3N_4 ceramics feature amorphous intergranular films (IGF) with a thickness of the order of 1 nm.[1–4] Clarke suggested a continuum model based on a balance of different forces leading to an equilibrium IGF thickness.[5] The major contributions in this model are the attractive van der Waals force, a repulsive steric force, and a potentially present electrical double layer force. It is expected that the magnitude of these forces is determined by compositional changes in the IGF, e.g., the concentration of cationic and anionic sintering additives. Since the composition of sintering additives strongly affects the mechanical properties of the ceramic[6] it is extremely desirable to understand the elemental distribution within the IGF, particularly that of the rare-earths used as sintering additives. This proved experimentally to be a very difficult task. With the advent of aberration-corrected STEM it seems now to become possible to characterize the detailed atomic structure in such localized IGF volumes using a fine electron probe with a diameter of less than 1 Å.[7–9] First results show that rare-earth dopants preferentially segregate to the (amorphous) film/(crystalline) grain interface.

Industrial interest in structural ceramics is to a large portion due to their excellent high temperature strength and creep resistance. Concluding high-temperature properties from data collected from quenched samples is dangerous, especially, since cooling rates attainable in most experiments are rather slow at temperatures above 1000 °C. It is important to study the behavior of these ceramics at the temperatures they are commonly applied at. However, up to now, only few TEM studies have aimed at investigating the high-temperature structure of IGFs in Si_3N_4, except for *in situ* conventional TEM experiments[10] and studies which use thinned TEM samples quenched from high temperatures.[11] Both fail to faithfully demonstrate the behavior of IGFs at elevated temperature at the atomic-level.

We will show that *in situ* HRTEM experiments are able to reveal the behavior of these materials at high temperature with atomic resolution,[12] reporting first experimental *in situ* HRTEM observations of the evolution of an IGF in Si_3N_4 at a temperature of about 820 °C.

* Corresponding author at: Erich Schmid Institute of Materials Science, Austrian Academy of Sciences, A-8700 Leoben, Jahnstraße 12, Austria.
E-mail address: zaoli.zhang@oeaw.ac.at (Z. Zhang).

0955-2219/$ – see front matter
doi:10.1016/j.jeurceramsoc.2011.03.016

2. Experimental methods

A silicon nitride (Si_3N_4) ceramic doped with 2 wt.% MgO + 7.2 wt.% La_2O_3 was used in this investigation. TEM samples were prepared by grinding, dimpling, polishing and ion milling as the final step. For ion milling an inclination angle of 12° was used. The Ar ion energy was in the range of 2.5–4.0 keV in a Gatan Duomill. The JEOL ARM 1250 microscope with a point-to point-resolution of 0.12 nm was used for the *in situ* HRTEM studies. The sample was suspended and heated using a Gatan double-tilt heating stage. The microscope is equipped with a drift compensation system, allowing the operator to stabilize the image and record photographs despite thermally induced specimen/stage drift.[13] The *in situ* annealing temperature in these experiments was about 820 °C. The specimen was held at this temperature for about 2 h, and was then cooled back to room temperature within a short time of typically 1 min. To minimize irradiation effects special care was taken when the images were acquired. The specimen was kept at low magnification and with the beam fully spread while being held at high temperature. All the HRTEM images were recorded with exposure times of less than 1 s, and under a defocus which corresponds to the minimum delocalization in this microscope.

3. Results and discussion

Fig. 1(a) shows the HRTEM image of two close Si_3N_4 particles before heating (the bright-field TEM image is inserted in the center). In the bigger particle, $\{1\,0\,\bar{1}\,0\}$ prism planes are parallel to the interface, while in the smaller one (~200 nm in size) these planes are inclined by 24°. The interface is very sharp and flat. It is obvious that an equilibrium amorphous IGF with a homogeneous thickness of about 1.0 nm exists and both prism planes are flat (the inset shows a diffraction pattern from these two particles, the prism planes of which are strongly excited). Fig. 1(b)–(e) shows the series of *in situ* HRTEM images recorded at elevated temperatures after different annealing times, which clearly show the evolution of the IGF with time. After 30 min the IGF starts to thin until it completely vanishes after 40 min. At the same time additional $\{1\,0\,\bar{1}\,0\}$ lattice planes appear in the interface region on the side of the bigger particle (marked by arrows in Fig. 1(b)–(f)), the number of which increases during the annealing treatment. The size of the smaller particle shrinks which becomes apparent by the shortening of the interface length (compare Fig. 1(a) and (f)). This can be clearly seen in the final stage of the two hours *in situ* annealing (Fig. 1(e)). In order to avoid the very fast drift during cooling (which took about 1–2 min) of the specimen the photograph shown in Fig. 1(f) was acquired about 10 min after having cooled back to room temperature. Note that one additional plane in the interface region has formed during the cooling, which is also found in quenching and annealing investigations.[8,14] Another noticeable feature is that the IGF has reappeared with a thickness of about 0.6 nm when the sample is observed at room temperature again.

In each of the Fig. 1(a)–(f) a cartoon illustrating the development of the additional planes with holding time has been inserted. These additional crystal planes slowly grow as the annealing proceeds and extend outside the IGF regions. Simultaneously the smaller particle shrinks. The appearance of additional crystal planes in the interface region is probably due to partial crystallization of the IGF during the time spent at high temperature. However, in contrast to previous observations[7,8] the crystallization of the IGF occurred at a relatively low annealing temperature. We also observe that the thickness of the IGF changes remarkably during *in situ* heating. With the software Digital Micrograph, the thickness variation of the nanometer-scale amorphous IGF was measured (Fig. 2). Obviously, holding the sample at high temperature causes a gradual decrease of the IGF thickness, making it disappear eventually, while atomic-level disorder may still be observed at the interface. Compared with the original value (approximately 0.9 nm), the IGF is thinner after cooling back to room temperature.

In order to understand the observed phenomena we will first discuss them in light of Clarke's model,[5,15] showing that our observations cannot be explained using a force balance model based on dispersion- steric- and electrical double layer forces. We will then propose a mechanism based on a changing IGF composition during annealing.

Of all the forces occurring in Clarke's model,[5,15,16] mainly the attractive dispersion force, Π_{disp}, and the repulsive electrical double layer force Π_{edl} have any significant dependence on temperature and may therefore initiate changes in the IGF thickness as the temperature increases. Once the thickness of the film changes the magnitude of all other forces is affected as well. Therefore, to completely evaluate the total force which the IGF is exposed to during heating, its relationship with temperature and IGF thickness must be established.

The attractive dispersion force can be written in the following form[5]:

$$\Pi_{disp} = \frac{H_{\beta g \beta}}{6\pi h^3}$$

h is the thickness of the intergranular film, the Hamaker constant, $H_{\beta g \beta}$, for the ceramic system can be expressed in a reduced form in case of a two-grain boundary as shown by Clarke, i.e., two Si_3N_4 grains separated by a siliceous amorphous film,

$$H_{\beta g \beta} = \frac{3}{4} k_B T \left(\frac{\varepsilon_\beta - \varepsilon_g}{\varepsilon_\beta + \varepsilon_g} \right)^2 + \frac{3\pi\hbar\nu_e}{8\sqrt{2}} \frac{(n_\beta^2 - n_g^2)^2}{(n_\beta^2 + n_g^2)^{3/2}} \quad (1)$$

where $\hbar$ is Planck's constant divided by 2π; ν_e is the absorption frequency, ε and n are low-frequency dielectric constant and the refractive index, respectively, of the phases β and g (here, bulk Si_3N_4 and intergranular film, respectively), k_B is the Boltzmann constant, T is the absolute temperature. By changing the dielectric constants ε and indices of refraction n of the phase β (crystalline) and g (amorphous IGF), the Hamaker constant $H_{\beta g \beta}$, and hence the attractive force across the grain boundary and the film thickness h are changed as well.

For simplicity, the investigated ceramic system is designated as the β-Si_3N_4–SiO_2–β-Si_3N_4. The corresponding parameters of β-Si_3N_4 and pure SiO_2 dielectric constant and refractive indices are adopted, which are 2.06 and 8.0 for Si_3N_4, 1.448 and 3.81 for SiO_2, respectively.[5] The electronic absorption fre-

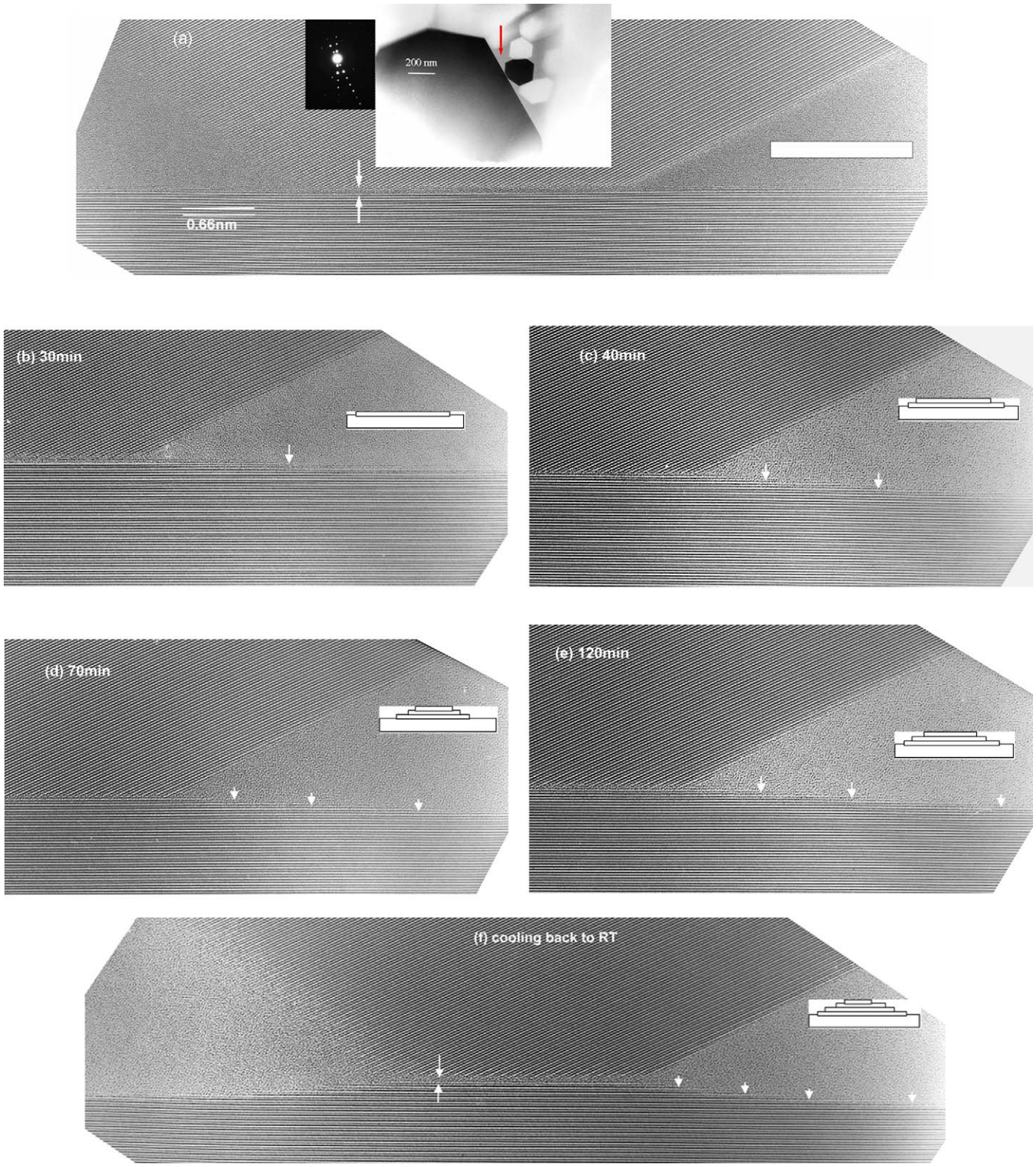

Fig. 1. HRTEM images of an amorphous IGF in Si_3N_4, (a) before heating, (b)–(e) time sequence images during *in-situ* heating at about 820 °C at different holding time. (b) 30min, (c) 40min, (d) 70min, and (e) 120 min. (f) was recorded 10 min after cooling back to room temperature. Note the thickness variation of the IGF with time. Please note that (b)–(e) only show half of the whole image. The bright-field image and corresponding diffraction pattern are inserted in (a). A red arrow in (a) indicates the position where HRTEM images were taken.

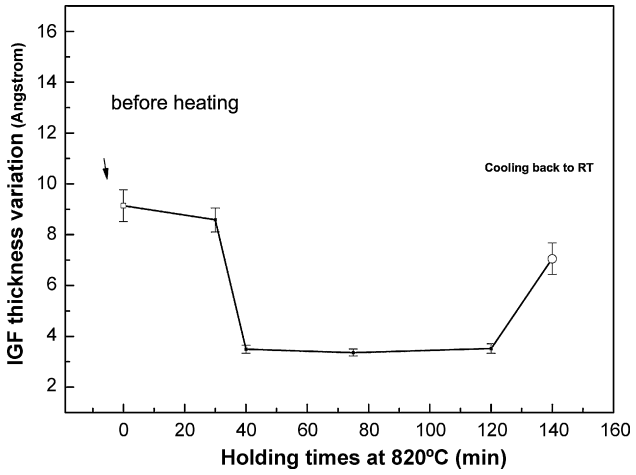

Fig. 2. Variation of the IGF thickness with holding time is displayed. For comparison the values before heating (the first point) and after heating (the last point) are also inserted.

quency is $\nu = 3 \times 10^{15}$ s.[16] Fig. 3(a) shows a three-dimensional surface plot of the dispersion force as a function of the IGF thickness (from the 0.6 to 1.4 nm) and temperature (from 300 to 2000 K). It indicates that the IGF thickness has relatively strong influence on the dispersion force. The linear temperature dependence of the dispersion force is shown enlarged in Fig. 3(b) for an IGF thickness of 0.9 nm. It varies by about 2% between room temperature (RT) and 1150 K. This effect becomes more pronounced at higher temperatures.

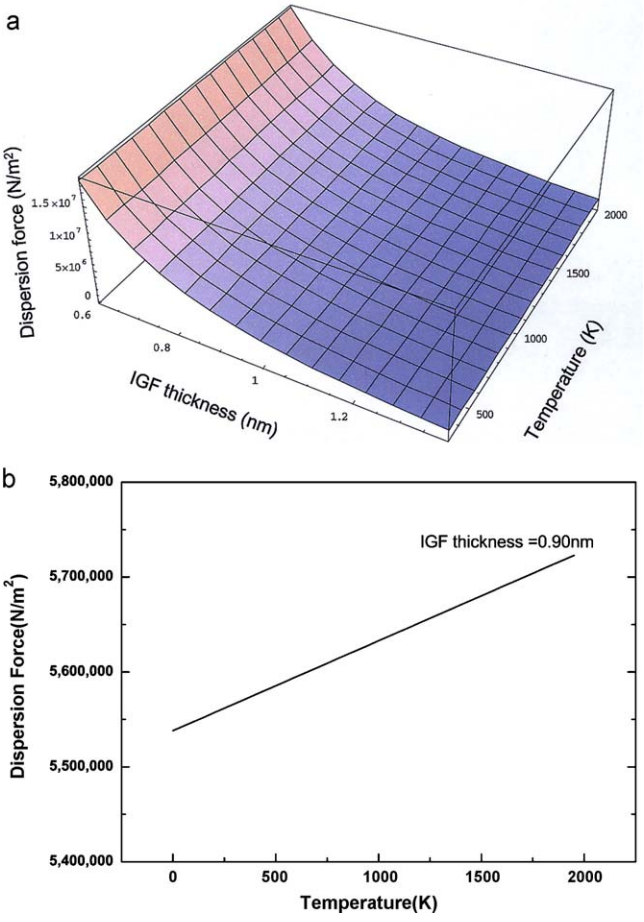

Fig. 3. (a) The estimated dispersion force variation with annealing temperature, from 300 to 2000 K, and IGF thickness from 0.60 to 1.4 nm. (b) Temperature dependence of the dispersion force for an IGF thickness of 0.9 nm, which is close to the experimental condition.

Using the weak overlap approximation for the force between charged parallel plates, the repulsive electrical double (EDL) force can be expressed by the following formula which also contains the temperature as a parameter[15,16]

$$\Pi_{edl} = \frac{64(k_B T)^2 \varepsilon\varepsilon_0}{(zeh)^2} \left(\tanh \frac{ze\psi_s}{4k_B T} \right)^2 \kappa^2 h^2 e^{-\kappa h} \quad (2)$$

with the Debye screening length $\kappa^{-1} = [(\varepsilon\varepsilon_0 k_B T)/(Nz^2e^2)]^{1/2}$

Here, e is the proton charge, ε is the dielectric constants of the intervening IGF, and ε_0 is the permittivity of free space, z is the ion charge, ψ_s is the electrostatic potential on the surfaces of the grains, N denotes the number density of mobile ions in the bulk, 5×10^{-3} (number/nm^3) is used in this system.[17] Based on the assumption underlying Eq. (2), namely a weak double-layer overlap ($kh > 1$), a relatively low surface potential can be suggested. In our estimation $\psi_s = 100$ mV is assumed. With appropriate parameters the EDL force between two grains can be calculated from Eq. (2). Its variation with IGF thickness and temperature is shown in Fig. 4(a). The increase of the EDL with temperature becomes less pronounced at high temperatures. Although the *relative* influence of the IGF thickness on the EDL force is stronger compared with the dispersion force, the magnitude of the EDL force is at least two orders of magnitude lower than the dispersion forces under the same conditions. Fig. 4(b) plots the dispersion force and the EDL force as functions of IGF thickness at 1150 K and a 100 mV surface potential. This shows how these two forces change as the IGF thickness shrinks during the annealing treatment.

These calculations show that the strongest temperature influence comes from the variation of the dispersion forces which tends to decrease the IGF thickness with increasing temperature. Although this is in accordance with our observations, it has to be noted that within the temperature range studied the variation of forces is so small that this can hardly be the main reason for the observed complete disappearance of the IGF, especially, since the repulsive steric force is proportional to exp $(-h/\zeta)$, where the screening length ζ is of the order of $\approx$3 Å.[5] We will therefore consider a different mechanism that may be responsible for the changes observed in our experiment.

From Fig. 1(a)–(e) it is can be seen that new $\{1\,0\,\bar{1}\,0\}$ crystal planes nucleate within the IGF and further grow, probably by a ledge mechanism, into areas extending outside the IGF region. At the same time, the length of the interface decreases, i.e., the smaller grain looses material at its sides. The tendency for lattice planes to nucleate at the larger grain within the IGF is obviously due to the proximity of the small grain. We believe that the newly forming $\{1\,0\,\bar{1}\,0\}$ planes have a composition close to Si_3N_4 because of the same spacing of the newly formed planes as the $\{1\,0\,\bar{1}\,0\}$ Si_3N_4 planes and because the atoms present in the amorphous phase (e.g., Lu, Mg) have a very low solubility within the Si_3N_4 lattice. While this fact alone might classify the

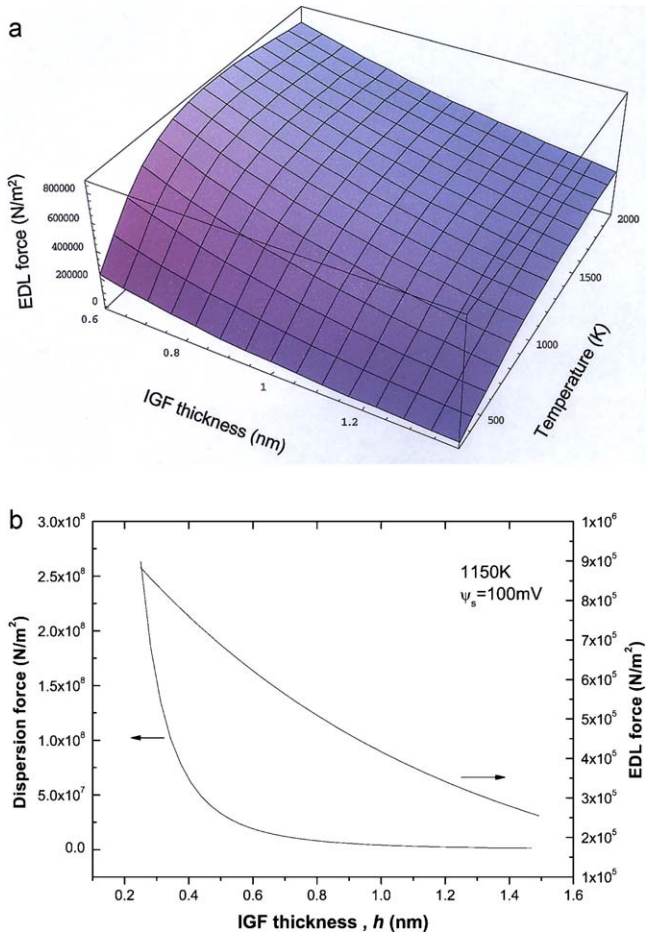

Fig. 4. (a) Electrical double layer (EDL) force as a function of temperature and IGF thickness. (b) Comparison of dispersion force and electrical double layer force at $T = 1150$ K and for a surface potential of 100 mV. Note that the dispersion force is several orders of magnitude larger than the electrical double force.

observation as a classical case of Ostwald ripening (the higher boundary curvature of the smaller grain gives it a higher, less favourable, surface energy density than the large grain), the apparent disappearance of the IGF cannot be explained by it. The crystallization of amorphous material to form new Si_3N_4 lattice planes can only occur, if its composition is close to that of the crystal. The atomic species, making up the IGF in its room temperature composition must either (a) concentrate at the IGF center, (b) diffuse along the IGF to the glassy pockets, or (c) spill over the top and/or bottom of the thin TEM sample. It is also conceivable that, despite the special care taken to minimize radiation damage, (d) certain elements have preferentially been removed from the glass by the high-energy electron beam. Any of the described scenarios (a)–(d) affects the composition and therefore the forces across the IGF, and ultimately, its thickness. In our case the interface is about 28 nm long and approximately 10–15 nm deep in the direction parallel to the electron beam. The scenarios (b) and (c), i.e., diffusion of certain species to the sides and spilling of amorphous phase to the top and/or bottom of the sample are therefore possible and, just from the distance argument, similarly likely. For larger interface areas the diffusion and/or liquid mass flow are less likely under otherwise equal circumstances. In confined systems, where mass flow is strongly inhibited, crystallization as observed in our experiment is also more difficult, since volume changes associated with the phase transformation give rise to strain energy.[18]

A simple entropic argument will easily discount possibility (a), the concentration of elements other than Si and N to the very center of the IGF. Scenario (d) may be the most likely, if it can be shown that La, O, and possibly Mg are removed more easily by the electron beam than Si and N. While Si and N have 4 and 3 bonds, oxygen atoms are only bound twice, and La atoms feel more comfortable at the Si_3N_4/IGF interface than in the center of the IGF.[7,9] Electron beam damage of the IGF may therefore preferentially remove the comparatively weakly bound oxygen atoms, leaving behind positively charged La^{3+}, Mg^{2+}, Si^{4+}, and N^{3+}, the latter 2 of which form Si_3N_4 (together with the material dissolved off the smaller grain). The remaining positively charged ions repel each other and move to the specimen surfaces and/or are also knocked out of the thin TEM foil by electron beam. The availability of equivalent low-energy sites makes knock-on electron beam damage less likely for crystallizing and already crystallized regions of the sample, leaving behind a (possibly just partially) crystallized IGF.

The re-appearance of the IGF while cooling back to room temperature may be explained in a similar fashion as its disappearance. Temperature induced compositional changes by diffusion and mass flow (possible explanations (b) and (c)) are reversible. The reduced IGF thickness after cooling down may be kinetically limited, i.e., a result of the relatively fast cooling rate, compared to the time it took the IGF to disappear. If radiation damage was responsible for the IGF thinning, diffusion from the glassy pockets must have filled the interface again. In ceramics containing neither magnesium, nor rare earth oxide additives Tanaka et al. found the IGF width to be (1.0 ± 0.1) nm,[2] which is significantly less than the with (1.6 ± 0.1) nm commonly quoted for La_2O_3-doped material.[3] Permanent removal of oxygen and the (by charge balance) corresponding amount of anions may have led to a different composition and thus a smaller thickness of the IGF after cooling down.

4. Conclusion

In summary, with *in situ* HRTEM it has been shown that an amorphous IGF can vanish at elevated temperature by the occurrence of additional crystal planes in the interface region during annealing, and that the IGF can reoccur after cooling back to room temperature. These results are different from the Clarke's[10] and Cinibulk's[11] observations, who claimed that no observable changes in the secondary phases at triple junctions or along grain boundary occur below 1000 °C. From the analysis of the forces assumed, according to Clarke's model,[5,15] to be acting upon the grains confining the amorphous IGF we concluded that their temperature dependence is too small to explain the variation of IGF thickness. Alternative explanations based on alteration of the IGF composition during annealing have been proposed. In addition, mass transport was observed to occur from smaller to larger grains.

Acknowledgements

We thank Ute Salzberger for the excellent TEM specimen preparation and Dipl.-Ing. Rainer Höschen for his help during the operation of the ARM 1250. We also thank Dr. A. Subramanian for helpful discussion. This work is financially supported by the EU under the contract G5RD-CT-2001-00586. In cooperation with NSF award DMR-0010062.

References

1. Kleebe H-J. Structure and chemistry of interface in Si_3N_4 ceramics studied by transmission electron microscopy. *J Ceram Soc Jpn* 1997;**105**(6):453–75.
2. Tanaka I, Kleebe H-J, Cinibulk MK, Bruley J, Clarke DR, Rühle M. Calcium-concentration dependent of the intergranular film thickness in silicon-nitride. *J Am Ceram Soc* 1994;**77**(4):911–4.
3. Wang CM, Pan X, Hoffmann MJ, Cannon RM, Rühle M. Grain boundary films in rare-earth-glass-based silicon nitride. *J Am Ceram Soc* 1996;**79**(3):788–92.
4. Schmid H, Rühle M. Structure of special grain-boundary in SIALON ceramics. *J Mater Sci* 1984;**19**(2):615–28.
5. Clarke DR. On the equilibrium thickness of intergranular glass phases in ceramic materials. *J Am Ceram Soc* 1987;**70**(1):15–22.
6. Satet RL, Hoffmann MJ. Impact of the intergranular film properties on microstructure and mechanical behavior of silicon nitride. *Key Eng Mater* 2004;**264–268**:775–80.
7. Shibata N, Pennycook SJ, Gosnell TR, Painter GS, Shelton WA, Becher PF. Observation of rare-earth segregation in silicon nitride ceramics at subnanometre dimensions. *Nature* 2004;**428**(6984):730–3.
8. Ziegler A, Kisielowski C, Hoffmann MJ, Ritchie RO. Atomic resolution transmission electron microscopy of the intergranular structure of a Y_2O_3-containing silicon nitride ceramic. *J Am Ceram Soc* 2003;**86**(10):1177–785.
9. Winkelmann G, Dwyer C, Hudson TS, Nguyen-Manh D, Döblinger M, Satet RL, et al. Arrangement of rare-earth elements at prismatic grain boundaries in silicon nitride. *Philos Magn Lett* 2004;**84**(12):755–62.
10. Clarke DR. High-temperature microstructure of a hot-pressed silicon nitride. *J Am Ceram Soc* 1989;**72**(9):1604–9.
11. Cinibulk MK, Kleebe H-J, Schneider GA, Rühle M. Amorphous intergranular films in silicon-nitride ceramics quenched from high temperature. *J Am Ceram Soc* 1993;**76**(11):2801–8.
12. Merkle KL, Thompson LJ, Phillipp F. Collective effects in grain boundary migration. *Phys Rev Lett* 2002;**88**(22):225501–4.
13. Phillipp F, Höschen R, Osaki M, Möbus G, Rühle M. New high-voltage atomic-resolution microscope approaching 1 Ångström point resolution installed in Stuttgart. *Ultramicroscopy* 1994;**56**(1–3):1–10.
14. Wang CM, Pan X, Gu H, Duscher G, Hoffmann MJ, Cannon RM, et al. Transient growth bands in silicon nitride cooled in rare-earth based glass. *J Am Ceram Soc* 1997;**80**(6):1397–404.
15. Clarke DR, Shaw TM, Philipse AP, Horn RG. Possible electrical double-layer contribution to the equilibrium thickness of intergranular glass-films in polycrystalline ceramics. *J Am Ceram Soc* 1993;**76**(5):1201–4.
16. Israelachvili JN. *Intermolecular and Surface Forces*. 2nd ed. London: Academic Press; 1992.
17. Estimation of total ionic concentrations in the amorphous phase: the composition of the original powder is 88.6 wt.% Si_3N_4 + 2 wt.% MgO + 7.2 wt.% La_2O_3 + 2.2 wt.% SiO_2. The amorphous phase is 11.4 wt.% of the Si_3N_4 ceramic system. The mole concentration for MgO and La_2O_3 are nearly 0.011 and 0.0049 mol/cm^3. The concentrations of Mg^{2+} and La^{3+} in the amorphous phase are about 6.62 and 5.85 (number/nm^3). The total ion concentration within the whole amorphous phase is estimated to be in the range of 1×100–1×101 nm^{-3}. Here, only La^{3+} is assumed to provide positive charges since there is enough experimental evidence that La segregates in the interface. It should also be noted that the above estimation is the ideal case. Considering the loss of additives and the very low percentage of the IGF in the total amorphous phase (IGF only is approximately 1–0.1% of the total amorphous phase), the number density of mobile ions (La^{3+} concentration) located in IGF is roughly in the order of 10^{-3}–10^{-2} nm^{-3}. In the calculation 5×10^{-3} nm^{-3} is used. The ion charge Z, though is +3.
18. Raj R, Lange FF. Crystallization of small quantities of glass (or a liquid) segregated in grain-boundaries. *Acta Metall* 1981;**29**(12):1993–2000.